出國報告（出國類別：開會）

2018 年第 44 屆國際微奈米工程研討會

服務機關：國防大學理工學院機械及航太工程學系
姓名職稱：李亞偉副教授
派赴國家：丹麥
出國期間：107 年 9 月 21 日至 9 月 29 日
報告日期：中華民國 107 年 10 月 04 日

摘要

國際微奈米工程研討會（International Conference on Micro and Nano Engineering）是歐洲歷史最為悠久的研討會之一，更是微奈米領域的 重要國際會議，現 每年於九月固定在歐盟各國輪流舉辦。本次 研討會在丹麥哥本哈根貝拉國際會議中心（Bella Center Copenhagen）舉行，議程則由丹麥科技大學（Technical University of Denmark）規劃，期程自 2018 年 9 月 24 起至 27 日止，鑑於以往細分多項專業領域導致議程過於分散，因此今年會議改善以往作法，將收錄論文概區分四類領域，俾利與會學者能充分參與討論。研討領域如下：一、微奈米工程方法與 製程（Methods and Processes），二、微奈米結構、元件與系統製造與整合（Fabrication and Integration of Structures, Devices and Systems），三、微奈米 物理化學原理與應用（Physical and Chemical Principles and Applications），四 、微奈米工程生活科學應用（Applications for Life Sciences）。

微奈米工程國際會議成立目的即在利用學術研討會模式，每年定期邀集世界各國微奈米工程領域研究學者和產業專業人士共同研討微奈米最新進展及其未來發展趨勢。自 1975 年以來，由於歷屆會議均由學術頂尖機構舉辦且論文審查制度嚴謹，因此 每年 會議 均吸引專業領域人士、期刊出版商與設備廠商與會，不僅 深受各國產學研機構重視，並獲 Elsevier 出版社長期贊助並擇優邀稿，成功提供一個專屬於微奈米工程創新技術發表與研究成果分享的學術平台。現今，隨著生活科技應用需求驟增，整合各領域專業導入微奈米工程研究尤顯重要；因此，舉凡微奈米創新製程、微奈米尺度電子熱傳、微奈米結構製造、微奈米元件製作與布局設計、微奈米藥劑開發與相關環境、生醫科學等均涵蓋在本屆會議研討範圍。個人此次以「YAG: Ce3 螢光材料最佳參數與特徵確定（YAG: Ce3+ Fluorescent Material Production and Performance Analysis）」為題進行發表，主要說明使用共沉澱法在不同沉澱攪拌轉速下合成鈰摻雜釔鋁石榴石（YAG：Ce）前驅體，另在控制不同煅燒溫度範圍加熱後，將所獲得的奈米粒子進行發光強度分析比較，確認其最佳製程參數。經與會學者提問討論，對於此一工程設計理論應用於多變因實驗作法，可兼顧研究成本與製程最適模式建立，可有效分析個別參數對性能之重要性，具有實用價值。

個人認為，學術交流經驗對於教學研究實屬重要，藉由參與國際會議與研究成果發表不僅可以觀摩最新研究成果、達到學術交流目的，亦可充分瞭解最新設備及製造技術發展訊息，增廣個人專業知識。個人有機會參與此一重要國際會議，首先感謝科技部專題計畫經費補助以及國防大學理工學院各項行政支援與研究教學設備支持，方能順利完成研究並彙整成果發表，後續更將秉持持續研究創新的積極研究態度，廣泛參與各項學術交流活動，以期在個人教學與研究品質方面有所助益。

目次

壹、會議目的

本屆 微奈米國際工程研討會（MNE 2018）在丹麥哥本哈根貝拉國際會議中心（Bella Center Copenhagen）召開，經嚴格審查篩選約 65%稿件後，共收錄來自 42 個國家 400 餘篇論文。會議研討重點計有工程方法與製程、結構、元件與系統製造與整合、微奈米物理化學原理與應用，與微奈米工程生活科學應用等；專業領域則涵蓋 微奈米工程 製程技術、光刻技術 、微機電與微光伏系統製造、元件設計、生活科學應用與 聚焦電子束誘導處理 等。會議成立迄今已達 44 年,隨著產學界重視以及會議論文品質不斷精進,現已成為 國際最重要且最具規模的微奈米領域專業會議 ,另由於會議發表論文多兼具實用與創新,因此相關研究成果不僅頗具學術價值,更能結合相關產業發展應用產品,普獲各國產學界矚目。有別以往區分領域與論文屬性規劃講廳方式,本次會議特別邀請知名學者連續二日進行單一場次專業演講,並另闢各議場供個別發表與自由研討。事實上,微奈米國際工程研討會成立目的在提供 微奈米工程 學術交流的專業平台,以發展相關技術增進各工程領域為宗旨;因此,為鼓勵產學界踴躍與會,會議均由學術頂尖機構主辦,廣邀專業設備商介紹先進機儀具,發表尖端製程技術。另本會議經年獲頂尖學術出版商與產業界贊助,更鼓勵各國產學研機構積極發展創新技術、引進合作,大幅提升微奈米工程實用價值。

為達產學交流目的,會議特設會場提供專業設備商與著名期刊出版社參展,不僅可以有效提供與會人士最新微奈米技術資訊、解決相關研究窒礙與技術可行性討論,並能同時提供各類研究論文發表優質期刊參考。個人認為,此一提升會議參與意願作法可供國內會議借鏡。

貳、會議過程

本屆會議自 9 月 24 日起至 9 月 27 日止,參與會議人士包含 30 餘國產學研專業人士,更不乏國際知名專業大廠,如台積電、鴻海、日立、三星電子等,共計收錄論文達 500 餘篇。經會議資料分析,方法與製程方面論文約收錄 220 餘篇,微奈米結構、元件與系統製造與整合約 110 篇,物理化學原理與應用約 150 餘篇,生活科學應用類則有 70 餘篇;相較往年多以生活科學應用為重點,本次會議投稿趨勢說明微奈米方法與製程相關研究正獲學術界重視。本屆會議自 9 月 24 日上午 0800 起開放報到並於當日 0900 時即正式開始議程,在短暫介紹國際知名學者與參展廠商後,大會主席丹麥科技大學 Anja Boise 教授特別介紹倫敦帝國理工醫學院生醫材料與重建醫學中心 M.S. Freng 教授,並邀請其針對相關奈米生醫領域發展現況發表最新研究成果。M.S. Freng 教授現帶領龐大研究團隊主持多項重大研究計畫,不僅著作等身、發表多篇 Science 與 Nature 等相關頂尖期刊,近年更致力於國際醫療互助及其生醫檢測研究,對於奈米尺度檢測技術尤為傑出。其報告指出,自組式奈米粒子生物傳感器具備獨特光學特性,可增強訊號傳遞能力,足以取代目前分析技術,對病理研究與臨床疾病檢驗成效發揮重大影響,因此已成為發展生物傳感器之優先選擇。眾多奈米粒子中,尤以膠體螢光和等離子奈米粒子對入射光會產生強烈響應,可將目標分析物有效連結,能在溶液環境中產生極佳靈敏檢測效果。近來,許多衍生研究聚焦於螢光量子點和等離子奈米金粒子等應用,甚或開發碳點、矽

點、上部轉換奈米粒子、合金等離子體奈米粒子以及奈米金/銀團簇等衍生感測材料，逐步發展可用於探測奈米粒子成核與生長之新穎工具。上述材料已成功運用諸如 微流體系統中精確合成奈米粒子、時間閥量子點螢光超靈敏檢測血清中癌症生物標誌物、使用超焠火奈米金粒子於多重細胞內感知訊息核糖核酸、利用智慧手機對分析物進行多重檢測，以及將奈米粒子生物傳感器與先進的 DNA／RNA 標靶進行系統整合等 生醫領域，且獲致顯著效益。另前瞻應用方面，M.S. Freng 教授認為合成具有優異物/化性的奈米粒子可實際導入遺傳研究分析、細胞傳感器和體內傳感器、即時檢測體內目標與結構之可視化等工具開發，另結合分子生物學、生物訊號學、數值模擬、生物工程和應用物理學等許多領域後，更可進一步發展大規模合成可重複式高質量奈米粒子生物傳感器技術。就奈米粒子生物傳感器在研究和診斷中的潛力而言，現已有多種方法能直接對粒子表面進行化學修飾，從而製備用於實驗室研究或臨床環境的特定粒子，使得它們可以針對標定分析物進行調整，並能為各式生物條件提供光學訊號，如此即可在複雜培養基或體內檢測生物訊號。

　　個人論文「YAG:Ce 螢光材料最佳參數與特徵確定」經大會歸類於「微奈米工程方法與製程」，排定於 9 月 25 日上午獲邀發表。本研究係使用共沉澱法，在不同沉澱攪拌轉速下合成鈰摻雜釔鋁石榴石（YAG：Ce）前驅體，並在 900-1300℃不同煅燒溫度下加熱，以獲得 YAG：Ce 螢光粉末。YAG：Ce 前驅體的最佳 Y/Al 化學計量比(3:5)是在前驅體混和液 pH 值為 7.7 的時候發生。實驗說明 YAG：Ce 相的結晶度隨著 沉澱攪拌轉速和煅燒溫度而提升，並且 YAG：Ce 螢光粉末的發光強度隨著煅燒溫度的升高而增 加，這是由於 YAG 相的結晶度較高。此外，在 900～1300℃的相同煅燒溫度下，沉澱攪拌轉速 400rpm 合成的 YAG：Ce 螢光粉末 在約 540 nm 處的最大螢光強度是以沉澱攪拌轉速 200rpm 合成的 YAG：Ce 螢光粉末的三至五倍; 這是因為在較高的沉澱攪拌轉速下製備的 YAG：Ce 前驅體混合溶液內產生均勻的流場，使其混 合溶液內 Y^{3+} 和 Al^{3+} 化學計量比較接近 3：5。研究說明不同沉澱攪拌轉速在相同鍛燒溫度下，其 發光性能差異三至五倍。因此，沉澱攪拌轉速對 YAG：Ce 螢光粉末的發光性能有相當大的影響。 AG：Ce 前驅體在不同的沉澱攪拌轉速下合成，然後在不同溫度煅燒得到 YAG：Ce 螢光粉末。 YAG：Ce 螢光粉末中 YAG 相的結晶度和 YAG：Ce 螢光粉末的 PL 發光強度隨著沉澱攪拌轉速和 煅燒溫度的升高而增加，但經分析比較其較高的沉澱攪拌轉速對發光強度有顯著影響，YAG：Ce 螢光粉末在 400rpm 下共沉澱並在 1300℃下煅燒時發光強度最佳，說明在此沉澱攪拌轉速時，混合溶液擁有均勻流場，導致 YAG：Ce 前驅體中 Y^{3+} 和 Al^{3+} 化學計量比趨近 3：5，YAG 相的結晶度提升，產生最高的發光強度。本研究源於國防科技不斷與時俱進，在各種武器設備上都需要相關照明及指示功能；並且在各種任務，諸如救災、演訓等等，照明及光源更是不可或缺。LED 不使用燈絲發光，所以沒有發熱、燒毀等缺點，其發光波長取決於材料能階，可涵蓋紫外線到紅外線波長範圍，現新型商用車輛多以 LED 作為光源選擇。LED 因為具備省電節能、環保、壽命長、體積小、抗震性佳、反應速度快及無污染等優點，故被稱為綠色光源，可廣泛應用於各種顯示、指示、裝飾、背光源、照明等不同用途。運用藍色 LED 混合 YAG：Ce^{3+}螢光粉發射黃光製備白色光源 LED 是目前公認效率最佳方式，其運用原理在於螢光粉受光刺激後，其內部電子會受激至高能階激發態，而當回復至原低能階狀態時，其能量會以光形式釋放外界，故可大幅提升 LED 光源亮度。本研究作法係採用「共沉澱法」備製 YAG：Ce^{3+}螢光粉，以碳酸氫銨作為沉澱劑，另加入硫酸銨作為分散劑，最後共沉澱得到 YAG：Ce^{3+}前驅體。在上述前驅體備製過程中，設定製程參數分別為攪拌速率及沉澱溫度，接續以不同煅燒溫度獲得 YAG：Ce^{3+}螢光粉

末，後續則藉由 XRD、FESEM、EDS 及 PL 等儀器針對 YAG：Ce^{3+}螢光粉末進行結晶像、粒徑、元素檢測及發光性能等分析，最後再以「響應曲面法」建立估測模型以求出最佳製程與控制材料粒徑等參數，完成開發適合軍事應用之低耗能、高效率之 LED 螢光材料設計。由於本研究經多次實驗驗證獲得優異效能，遂引起在場許多學者詢問製程方法，並對研究構想多有鼓勵及肯定，使個人體認學術研究唯有結合實務應用層面方能展現其工程價值。針對於上述最佳參數確定方法，日本小糸製作所 Hisayoshi Daicho 研究部研究員等人認為利用建立發光性能多因子參數方程，可以大幅簡化奈米粒子在製程中所產生的未知熱化學效應及其與旋轉流場間之多重物理偶合關係，以取個別參數一次偏微分為零方式即可獲得最佳/差參數設定值。有鑑於確定溫控範圍可避免熱聚集造成持續高溫導致奈米粒子聚集，因此本研究對製作均質化螢光粒子而言，適時提供一種合理參考依據。本會議論文歷經同儕審查與篩選後，個人投稿論文現已獲得微電子工程期刊（Microelectronic Engineering）通知邀稿，刻正準備中。

9 月 26 日議題置重點於「微奈米結構、元件與系統製造與整合」與「微奈米工程生活科學應用」等。在諸多報告中，其中尤以喬治亞理工學院 Yogendra Joshi 教授針對微流體操控技術應用在熱傳元件方面研究令人深刻。其報告指出，應用操控微流體方式在提升電化學反應與生醫檢測效能方面已逐漸成為趨勢；而在諸多操控方法中尤以利用磁性流體力學所發展的加速流場混合機制的作法最受矚目。由於電磁感應具備設計簡單與可持續操控特性，僅需在系統外部施加磁場，磁性流體便會產生誘導電場造成勞倫斯力使流場擾動，進而提升熱擴散能力。此外，更可藉由電場設計誘發磁場降低流場重力、黏滯力等影響而強制改變流場行為，故使得相關發展之主動、半主動式微型混合器應用範圍大幅擴增。有鑑於此，因應機電工程發展日新月異，結合學理研究發展多樣化熱管理技術更顯重要。基於既有研究基礎上，應用磁性流體可操控性研製能處理時變熱源的散熱元件，以使機電設備能有效避免瞬間或長期高熱負載造成內部組件熱應力集中等影響，將是可供深入研究之議題。機電設備熱管理目的在有效率地移除工作廢熱，使裝置內部元件能在可接受之操作溫度下作業，因此如何使其能長期維持正常運作則為熱管理的重要指標，相關熱管理技術反應至一般設計層面包括高熱傳輸能力、低熱阻值、以及具備長效期可靠度、構型微小化與低成本等要求，通常以水/氣冷方式即能達到散熱功效，然而對於在複雜、嚴苛環境中使用的高功率機電子設備而言，在操作條件限制下往往無法以一般傳統方式進行內部散熱，因此在最低成本考量下，應針對高功率機電設備發展一款新穎的熱管理機制，以有效控制裝備作業溫度，提升整體可靠度。Yogendra Joshi 教授等人研究係以簡單迴路設計一款被動式散熱元件，具備製作簡單、熱效率高，可因應熱源位置與熱通量大小而變化構型，以及對操作環境適應力佳等特性，另搭配模組設計整合風扇、均溫板、鰭片等輔助件，可視目標需求規劃成系統套件，能普遍應用於各式電子與機電設備中；諸如個人電腦、核電廠控制機組、或是太空載具等，皆能實際運用且符合設計需求。由於迴路可以獨立操作、環境適應力佳，並具備低熱阻、操作範圍廣與可彈性延長熱傳輸距離等優點，且迴路設計會產生離心力迫使管路中心附近區域流體與管壁附近流體交互作用，周而復始地在垂直軸向速度場的平面上產生對稱渦流，使得熱傳與質傳效率遠高於相同流量與加熱條件下之直管流，因此適合應用在高熱通量熱源之散熱設計，相信隨著工程技術不斷創新，未來發展潛力勢必難以限量。經個人提問並與演說者討論後，認為機電設備內部熱源多半隨著構型設計、操作時間或環境條件而有所變異，其產生之熱通量並非為一固定值，因此熱管理應用方面必須考慮整合跨領域先進技術，方能因應預期可能衍生之窒礙。於此，考慮周期性、固定範圍振盪與瞬間陡升條件下規劃控制熱源變化，以迴路布局配合蒸發器熱負載設計，並以外加磁場、引用可視化實驗等多種研究方法等深入探討磁性流體擾動與熱擴散之時變關係，當可完整瞭解磁流耦合效應（對兩相流共軛熱傳效率之增益，進而發展一款能應用於時變熱源的散

熱元件。

　　會議最後一天，由美國桑迪亞國家實驗室資深研究員 Theron M. Rodgers 針對金屬積層製造技術發表演說，此一技術發展正符合我國推動工業自動化與精密製造相關。金屬積層製程源於 3D 列印技術，現已掀起新一波產業革命，是具有效率、免開模、低成本、客製化等功能，其製程方式不僅顛覆傳統機械模具技術，對於複雜、精微結構製造亦具有一體成型製作潛力，備受研究及產業單位界矚目，已成為各國努力投入發展的主要技術，因而正積極規劃投入積層製造核心關鍵技術開發，被視為具有帶動製造產業轉型與創新產品的潛能。金屬積層製程近來發展迅速，衍生諸如雷射束熔融、電子束熔融、雷射金屬沉積等方法，惟仍受制於製作速度與尺寸限制等缺點。直至 2017 年，中國大陸西安交通大學 J. Du 教授等人提出將金屬融合鍍層後，再利用雷射熔融成型的熔合鍍層方式成功克服上述缺點。此方法不僅可在短時間內製作大尺寸金屬零件，更能兼顧均質與輕量、強固航太組件設計原則。鑑於金屬積層製程可解決傳統機械加工無法克服的問題，許多產業已投入開發使用相關技術取代傳統機械加工。另隨著材料加工技術創新，目前金屬積層製造已可應用多種材料製造大型零件等，近期更成功導入航太產業。Theron M. Rodgers 即以開發自主無人飛行載具機翼微結構積層製造技術為題，說明利用金屬積層製程實現機翼輔助結構設計與製作技術，以降低合金用量且積極改善一次性金屬成型技術限制，在航太結構研究而言相當具有原創性。一般機翼外形氣動力研究甚多，不同飛行速度需求所應匹配之最佳機翼外形亦早有定論，然機翼內部結構及其負載支撐能力等研究仍略嫌不足。事實上，機翼結構影響飛行器氣動力甚鉅，傳統機翼構型採多種另組件組合設計，不僅設計複雜、重量控制不易且易受外在氣動力造成共振，誘發機翼疲勞。然而，無人飛行載具強調重量輕、體積小，因此在輕量化要求下尋找最適結構並發展其製程對策當是設計重點。相較於大型飛行載具重量足以克服局部氣流變化，無人飛行載具則必須在重量限制下考慮滯空條件，從而限制其飛行速度與使用範圍。因此，為提升無人飛行載具飛行效能，設計著重在利用金屬積層製程技術開發一款質輕、高抗震性、製程簡易之微型機翼結構設計，並以高強度、均質化一體成型蜂巢結構取代傳統組合式構型，從內部機械結構著手改善機翼氣動力表現，期能在可改變機翼外在撓性下有效提升機翼內結構剛性，避免因結構受力不均造成局部應力集中而影響整體氣動力特性，以能有效利用結構剛/撓性抵銷機翼表面氣流場所造成的不穩定負載，使機翼能在一安全模態下振動，不致造成結構變形、疲勞甚或破壞。另由於組成機翼之內嵌結構形狀與大小一致，不僅利於生產程序簡化與局部維修，亦有助減省生產、維修成本。現階段大多數無人飛行載具整體結構製作方式仍是利用傳統機械製程為主，耗時費工且誤差偏高，然利用數位直接製造三維成形技術開發固有應變法形變量理論預測模型並輔以因子設計法於機翼內部微結構設計、透過雷射金屬積層製程與材料實驗參數調控，進行開發自主無人飛行載具機翼強固結構研製，最後以參數優化方式逐步設計一體成型式內嵌蜂巢模組，此役並結合成完整機翼結構。其研究結果符合航太認證規格，未來將應用於先進航太與國防製造產業，達成結構強固與輕量化零組件開發目標。個人認為，飛行載具外型設計以臻一定標準，惟機件系統整合或因應操作環境所產生之不可預期影響（如振動、應力殘留等）仍需發展關鍵技術克服重點。配合我國國機國造政策，

參考此一技術正可突破現有結構設計瓶頸，在確保品質與時程基礎上達成精密複雜機組件開發。

　　會議場地分布於貝拉國際會議中心一至三樓層，並依據研究領域劃分二大型會議廳、三海報展場、二大型交誼廳與多個小型簡報室及預備室，不僅各項軟硬體支援充分，同時提供詳細報告議程與提醒通知 APP，使與會人士可以輕鬆進行研討交流，避免因會議議程緊湊而有所疏漏。此外，大會會議最後一日下午更邀請哥本哈根科技大學多名教授主動參與座談研討，使專業領域相近學者可以進一步針對研究議題相互討論，提供未來研究方向意見。個人近年已發表多篇微奈米工程相關論文，包括奈米壓印圖樣製作、微奈米流體蓄/釋熱系統開發以及微泳器操控特徵研究等，雖然研究具備多樣性與實用性，但仍有許多進階研究尚待驗證測試，所幸藉由此一難得機會可直接與國際著名學者請教，不僅立即獲得許多關鍵資訊，更透過交換電郵方式可於日後學術交流，深感不虛此行。討論議題中，多位學者均對微型系統缺陷檢測技術甚感興趣，深感機構設計必須因應規格需求考慮材料選用與組件布局，方能在正常操作環境下維持一定可靠度。個人認為，非破壞檢測設備雖然可直接、快速檢查系統缺陷，然其固定性與檢測範圍侷限性以致難以攜行而使應用層面受限。個人提出可將系統識別理論導入錯誤診斷技術開發，如此即可利用外施物理量方式將量測數據建立時域診斷模式,藉由輸入/出因果關係比對差異性。此外，經轉換頻域模式並獲得頻率共振特徵圖譜後，更可利用能量傳遞觀點探討缺陷影響。此一整合控制領域方法，不需搭配高階設備即可發展可攜式裝置進行初步檢測工作，均得到在場學者肯定。研討過程中，許多學者深感各國不斷追求經濟發展，但在急速工業化與城市化之際，伴隨此一經濟發展而來的卻是水土、林木、能源等資源日趨消耗殆盡，導致環境生態問題日益嚴重，衍生諸如臭氧層破壞、溫室效應、有害廢棄物運輸與存放等難以回復的環境污染問題。在眾多污染中，尤以空氣污染物會藉由氣流擴散、地形隔絕、化學反應等因素造成成分、濃度變異，難以預測控管，因此期許能應用奈米科技發展可針對細微污染物進行靈敏檢測與即時防制技術，深獲在場學者熱烈支持，相信此議題當是未來研究重點。

參、會議心得

　　隨著各國經濟持續增長，科研發展遂成為先進國家產業競爭力指標，而教育正是確保國家競爭力之基石。鑒此，個人深切認知唯有隨時充實本身專業能力與研究能量，方能維持自身競爭力並能帶領學生鑽研新知。首先感謝科技部經費補助以及國防大學理工學院行政支援與研究教學設備支持，方使個人有機會參與此一會議。

　　經概略分析議程內容與大會簡報，發現亞太地區國家參與本會議呈逐年增加趨勢，不僅論文發表數量與品質大幅提升，參與師生團隊亦相對龐大，足見亞太地區學術科研能力實不容小覷。事實上，藉由參與國際重要會議不僅有助推廣國家學術研究能力，同時也可提升學校與個人知名度，因此許多知名學者藉由參加本會議以作為交流平台，不僅展示其創新研究成果更藉此獲得許多產業合作機會，進而結合學術與實務開發應用技術。除歐洲各國眾多學者參與外，日本與中國大陸兩國學者與會人數最多，其次則為南韓，而國內則包括清大、交大、台師大、北科大、聯合大學與本校等學者與會；相較之

下，國內發表論文不乏產業界與研究機構共同參與研究，顯見產學合作儼然已成科研發展潮流。

　　本屆會議舉行地點為譽有設計之都美名的丹麥首都哥本哈根，市區內三所甚具規模大學均世界聞名。經與丹麥學者言談中發現，丹麥大學著重啟發式教育，因此課程偏重觀念教授、內容廣泛紮實，上課時師生互動程度高，學生自主性強且視大學教育為職前投資，因此學習意願高昂，反觀我國學生相對保守的學習態度而言，實在值得藉鏡。此外，各校研究風氣與研究規模均足以支撐各項計畫，不僅經常承接跨國計畫，同時持續性進行人才交流，有助於拓展研究層面亦有助於提昇跨領域技化管理能力。個人認為，培養主動積極的學習態度源於對求知的渴望與熱忱，因此如何激勵學生投入研究與學習當是本校國防科研人才培育重點。個人會彙整本次會議心得並將此一難能可貴交流經驗利用輔導課程期勉本系同學，以激勵其學習熱忱並建立積極正面的學習態度。

　　本會議普受專業人士推崇，現已是微奈米工程領域最重要會議之一，近來參與人數與投稿件數雖不斷增加，但在嚴謹審查機制篩選下，均維持限定額度論文數量，會議品質廣受產學界肯定。就參與本次會議經驗而言，個人深切體認必須持續精進研究能力，並在現有基礎上不斷創新、拓展研究領域，以在既有基礎上逐漸累積研究能量。另透過會議交流可以相互觀摩最新研究成果，能直接與專家學者交換研究意見作為參考，同時也有助於個人學術溝通能力提升、對自己研究工作更深具信心。

圖一、貝拉中心會場及會議報到處、設備商與展示區
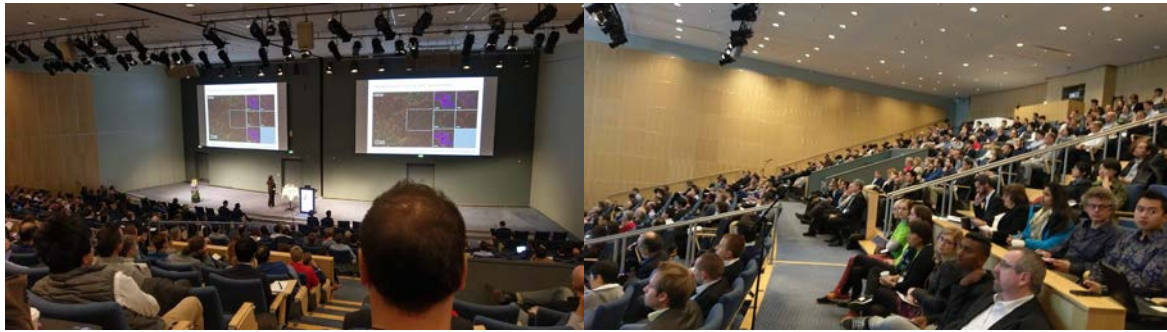
圖二、議程論文發表現場

肆、建議事項

一、本次會議無論議程安排或各項軟硬體設施均十分完善，在產業界支持下，會場展示許多新式先進製程與量測設備，使與會學者獲益匪淺。建議國內相關工程研討會除邀請專家學者與會外，亦能積極廣邀產業界共襄盛舉，不僅可以提供學者研究參考，同時可有助於促進產學合作。

二、「工欲善其事，必先利其器」，考量貴重設備使用侷限性，建議可跨系所整合研究資源、統合研究能量，甚或採用校際策略聯盟方式結合各院校專才，如此方能具備規劃跨領域、大規模整合計畫能力。

三、建議可規劃重點研究議題進行校際合作，藉由定期研討交流，逐步發展長期合作模式，提升整體研究能量。

四、建議在研究所課程規畫方面，可加強英文學術寫作與簡報等相關課程，以培養研究生具備良好學術表達能力。此外，鼓勵老師及研究生參加國際學術研討會，瞭解先進國家最新研究趨勢，以增進國際觀並達學術交流目的。

計畫編號	MOST 106-2218-E-606-007-MY2
發表論文題目	YAG: Ce3 螢光材料最佳參數與特徵確定 YAG: Ce3+ Fluorescent Material Production and Performance Analysis
出國人員姓名 服務機關及職稱	李亞偉　Lee, Ya-Wei 國防大學理工學院機械及航太工程學系 副教授
會議時間	自民國 107 年 09 月 21 日起至民國 107 年 09 月 29 日
會議地點	丹麥　哥本哈根
會議名稱	中文：第 44 屆微奈米國際工程研討會 英文：the 44th International Conference on Micro and Nano Engineering (MNE2018)

伍、發表論文

Determination of optimum parameters and characterization of YAG:Ce fluorescent material

Ya-Wei Lee[a], Hung-Hua Sheu[b], Chih-Cheng Chou[c], Su-Hsen Wu[a]

[a] Department of Mechanical and Aerospace Engineering, Chung Cheng Institute of Technology, National Defense University, Taoyuan, 335, Taiwan
[b] Department of Chemical and Materials Engineering, Chung Cheng Institute of Technology, National Defense University, Taoyuan, 335, Taiwan
[c] Department of Power Vehicle and Systems Engineering, Chung Cheng Institute of Technology, National Defense University, Taoyuan, 335, Taiwan

Abstract

The quality of YAG:Ce phosphors will influence the luminescent performance of white LEDs devices. Therefore, in this study, we attempted to synthesis high quality YAG:Ce phosphors using coprecipitation method. YAG:Ce precursors were synthesized through coprecipitation at different rotational speeds of an electromagnetic stirrer and then heated at different calcination temperatures ranging from 900 to 1300 °C. X-ray diffraction analysis revealed that phase-pure phosphors could be obtained from the precursors synthesized at 400 rpm and then calcined at 1300 °C. The emission intensity of Ce-doped YAG phosphor increased with the calcination temperature, owing to the higher crystallinity of the YAG phase. Moreover, at the same calcination temperature from 900 to 1300 °C, the maximum fluorescence intensity at approximately 540 nm of the YAG:Ce nanopowders synthesized at 400 rpm increased three to five times that of the YAG:Ce nanopowders synthesized at 200 rpm. The optimal luminescence performance of the YAG:Ce nanopowders was obtained at 400 rpm and at a calcination temperature of 1300 °C. The results of luminescence performance indicated YAG:Ce nanopowders has a great potential for development of white LEDs devices.

Keywords: YAG:Ce nanopowders, Y/Al ratio, rotational speed

1. Introduction

In the development and application of "white light" light-emitting diodes (LEDs), trivalent cerium-activated yttrium aluminum garnet (YAG:Ce) nanopowders are among the most important phosphors because YAG:Ce^{3+} nanopowders are suitable for converting the blue LED radiation into a broadband yellow emission [1-3]. The quality of YAG:Ce nanophosphors, such as purity and particle size, affects the brightness and efficiency of white LEDs. Therefore, synthesizing high-quality YAG:Ce phosphors is important.

YAG nanopowders doped with activators can be mainly synthesized by several wet chemical methods such as solvothermal synthesis [4-6], hydrothermal synthesis [7-9], coprecipitation [10-12], and sol–gel combustion [13-15]. In general, the synthesis of YAG nanopowders by using chemical techniques can result in homogeneous mixing of the precursor materials at a molecular level, thereby lowering the synthesis temperature and

promoting the formation of submicron and/or nanosized particles having uniform grain morphology. Among the aforementioned wet chemical processes, the coprecipitation method is a relatively simple approach to preparing YAG nanopowders with a pure phase, homogeneous chemical composition, and high crystallinity [16-18]. Therefore, the coprecipitation method was used to synthesize YAG:Ce nanopowders in this study. The factors affecting the quality of YAG nanopowders synthesized using the coprecipitation method include the precipitant concentration [19,20], precipitant type [21-24], and reaction temperature [25,26]. A previous study indicated that in the coprecipitation process, the rotational speed of the electromagnetic stirrer affects the uniform mixing of solutions and also the particle size of Nd:YAG nanopowders [27]. However, the effect of this speed on the optical characteristics of YAG nanopowders doped with rare-earth elements such as neodymium, ytterbium, and cerium has seldom been investigated. Therefore, we selected YAG:Ce phosphors as the study material to investigate the effect of the rotational speed of the electromagnetic stirrer on the luminescence of YAG:Ce nanopowders. In this study, YAG:Ce precursors synthesized at different rotational speeds of the electromagnetic stirrer during the coprecipitation process were calcined at various temperatures to obtain YAG:Ce nanopowders. The luminescence property of the YAG:Ce nanopowders was analyzed using a fluorescence spectrometer, and the effect of the rotational speed of the electromagnetic stirrer on the luminescence property of the YAG:Ce nanopowders was studied.

2. Experimental

2.1 Materials

The raw materials used in the synthesis of YAG:Ce nanopowders were yttrium nitrate hydrate ($Y(NO_3)_3 \cdot H_2O$, purity > 99.9%, Alfa Co. Ltd.), aluminum nitrate hydrate ($Al(NO_3)_3 \cdot H_2O$, purity > 99.9%, Sigma-Aldrich Co. Ltd.), cerium nitrate ($Ce(NO_3)_3 \cdot 6H_2O$, purity > 99.9%, Alfa Co. Ltd.), and ammonia bicarbonate (NH_4HCO_3, analytical reagent, purity > 99.9%, Sigma-Aldrich Co. Ltd.). The starting solutions were prepared by dissolving the corresponding raw materials in deionized water, followed by filtration.

2.2 Coprecipitation process

$Y(NO_3)_3 \cdot 6H_2O$ and $Al(NO_3)_3 \cdot 9H_2O$ were dissolved in deionized water with a molar ratio of 3:5 to obtain a mixed solution in which the concentration of both Y^{3+} and Al^{3+} was 0.5 M. The composition of doped cerium was maintained at 0.05 at.%. The precipitating agent was prepared by dissolving analytical grade NH_4HCO_3 in a mixed solvent of alcohol and distilled water. The precipitating agent was dripped into the mixed solution at a rate of approximately 30 mL/min, controlled by a peristaltic pump at different rotational speeds of the electromagnetic stirrer (200, 300, and 400 rpm). The suspension was aged for 48 h, filtered, and then washed with distilled water and alcohol to obtain the precipitate. The precursors were produced after the precipitate was dried at 90 °C for 48 h in a dryer. The obtained precursors were sieved through a 200-mesh screen and then air calcined at various temperatures from 900 to 1300 °C for 2 h to yield pure YAG:Ce nanopowders.

2.3 YAG:Ce nanopowder characterization

The YAG:Ce nanopowders prepared under the same conditions were divided into three samples for various analyses. Phase identification of the YAG:Ce nanopowders was performed using an X-ray diffraction (XRD) system (Model D2 PHASER, Bruker, Germany). The X-ray radiation source used was Cu Kα, and the diffractometer was operated at 40 kV and 100 mA. The microstructures of the YAG:Ce nanopowders were analyzed using a field-emission scanning electron microscope (Model JSM-6700F, JEOL, Japan). The YAG:Ce precursors were coprecipitated at various rotational speeds of the electromagnetic stirrer and then calcined at different temperatures from 900 to 1300 °C. The chemical composition of YAG:Ce after calcination at 1300 °C was analyzed using an electron probe X-ray microanalyzer (JEOL JXA-8200, Japan) across five measured positions for each sample. Finally, the photoluminescence spectra of the YAG:Ce nanopowders were analyzed using a fluorescence spectrophotometer (Brookhaven, NanoBrook 90Plus, U.S.A.) at room temperature. The fluorescence intensities of the YAG:Ce nanopowders prepared in this study were compared with the fluorescence intensity of commercial YAG:Ce phosphors (Nemoto & Co. Ltd., Japan). The flowchart of the coprecipitation process is shown in Fig. 1.

3. Results and discussion

YAG ($Y_3Al_5O_{12}$) has a chemical stoichiometry of Y^{3+} and Al^{3+} equal to 3:5. During coprecipitation, the Y/Al ratio within the precursors considerably affects the transformation of the pure YAG phase after calcination. Marlot et al. [28] reported that precursors prepared at final suspension pH values between 7 and 7.4 during the coprecipitation process can result in a single YAG phase after calcination at 1100 °C. Moreover, the YAG nanopowders contain impurity phases such as yttrium aluminum monoclinic (YAM; $Y_4Al_2O_9$) and Y_2O_3 when the precursors are synthesized at pH values higher than 7.4. Sang et al. [29] indicated that precursors aging at high pH values result in a change in the Y/Al ratio within the precursors and an increase in the impurity content of the calcined powder. Therefore, in this study, we analyzed the chemical composition of Y and Al of the calcined YAG powder, the precursors of which were synthesized at different final pH values (6.2, 7.3, 7.7, and 8.0) of the suspensions. The experimental results are presented in Fig. 2, indicating that the Y/Al ratio of the precursors calcined at 1100 °C was the closest to 0.6 when the final pH values of the suspensions were maintained at 7.7. In this study, to obtain a pure YAG phase nanopowder, the final pH values of various mixing solutions were controlled at 7.7 during the coprecipitation process. In addition to the final pH values of the suspensions, the rotational speed of the electromagnetic stirrer is an important factor affecting the purity of YAG nanopowders. Therefore, we investigated the effect of the rotational speed of the electromagnetic stirrer on the formation of a YAG phase during the coprecipitation process. Fig. 3 illustrates the relationships between the average Y/Al ratios of the YAG:Ce precursors synthesized at various stirrer rotation speeds and calcination temperatures. The average Y/Al ratios of the YAG:Ce precursors coprecipitated at 200 rpm and then heated at calcination

temperatures ranging from 900 to 1300 °C were 0.63, 0.72, 0.67, 0.72, and 0.8. The average Y/Al ratios of the YAG:Ce precursors heated at the various temperatures deviated considerably from the standard Y/Al ratio of 0.6; this can be attributed to the YAG:Ce precursors being prepared under uneven coprecipitation conditions. The distribution curves of the average Y/Al ratios of precursors coprecipitated at various electromagnetic stirrer speeds and then heated at different calcination temperatures revealed that an average Y/Al ratio relatively close to 0.6 was associated with stirrer speeds from 300 to 400 rpm. However, the distribution curves of the YAG:Ce Y/Al ratios deviated substantially from the standard Y/Al ratio of 0.6 when the stirrer speed was 500 rpm. The optimal Y/Al ratio curve (closest to 0.6) occurred at 400 rpm. A suitable stirrer speed results in a homogenous mixing process and thus the precipitation of homogenous YAG:Ce precursors with a Y:Al stoichiometry of 3:5. Generally, in ionic liquid systems, the reaction rate and homogenization of mixing solutions are affected by the stirrer speed. Regarding graphical representation, the relationship between the reaction rate of mixing solution and the stirrer speed appears as a "volcano-plot," because the reaction rate of solutions decreases with increasing stirrer speeds after a certain critical stirrer speed [30]. In this study, the relationship between average Y/Al ratios and stirrer speeds agreed with the relationships reported in the cited studies.

Fig. 4 presents the XRD patterns of the YAG:Ce precursors synthesized at different rotational speeds of the electromagnetic stirrer and then calcined at 1300 °C. The precursors synthesized at an electromagnetic stirrer rotational speed of 200 rpm and then calcined at 1300 °C exhibited the coexistence of YAG and YAM ($Y_4Al_2O_9$) phases; the XRD angles were observed at 2θ = 12.1°, 19.6°, 26.8°, 29.3°, and 30.8°, indicating the existence of a YAM phase. The diffraction intensity of the YAM phase only presented in the precursors synthesized at 200 rpm and calcined at 1300 °C. The diffraction intensity of the YAM phase decreased concurrently with increases in the stirrer speed from 200 to 400 rpm and disappeared for the precursors synthesized at 300 and 400 rpm and calcined at 1300 °C. However, the diffraction peaks of the YAM phase reappeared for precursors synthesized at 500 rpm and calcined at 1300 °C. These findings suggest that the range of 300–400 rpm was the optimal stirrer speed for supporting homogenous mixing and chemical reaction in the coprecipitation process. The YAM phases disappeared because suitable rotational speeds (300–400 rpm) facilitated a sufficient chemical reaction in the mixed solution to obtain homogeneous precursors and thereby achieve chemical stoichiometry of the Y:Al ratio after calcination. The precursors calcined at 1300 °C transformed into a pure YAG phase when the stirrer speed was in the range of 300–400 rpm. When the stirrer speed increased to 500 rpm and the mixture was calcined at 1300 °C, the XRD diffraction peaks that represented the YAM phase reappeared. Compared with the results in Fig. 3, the XRD results indicated that the chemical composition of the precursors was relatively homogenous in mixing solutions stirred at 400 rpm and in a nonhomogeneous mixing condition stirred at 500 rpm during the coprecipitation process.

Fig. 5 shows the XRD patterns of all samples prepared at different rotational speeds of the electromagnetic stirrer and then heated at various calcination temperatures. The intensity of the main diffraction peak (420) increased with an increase in the calcination temperature and in the rotational speed of the electromagnetic stirrer from 200 to 400 rpm. These increases corresponded with an increase in the YAG phase, indicating the improved crystallinity of the YAG:Ce nanopowders. Therefore, to determine the relationship between the crystallinity of the YAG:Ce nanopowders and the stirrer speed, and the calcination temperature, the intensity of the main diffraction peak (420) of the YAG:Ce nanopowders prepared under various conditions must be calculated. To set a standard, the precursors synthesized at different rotational speeds of the electromagnetic stirrer were calcined at 1300 °C for 2 h. The integrated intensity of the strongest reflection peak (420, 2θ approximately 32.01°–34.44°) was observed in the YAG:Ce precursors coprecipitated at 400 rpm and heated at 1300 °C; this highest integrated intensity was used to define the 100% level of the standard. The crystallinity levels of the YAG:Ce precursors calcined at various temperatures for 2 h were then determined by comparing the integrated intensity of the maximal reflection (420) with the YAG:Ce nanopowder standard. The crystallinity (C%) levels of the YAG:Ce precursor samples calcined at various temperatures for 2 h were calculated using the following equation:

$$C\,(\%) = \frac{I_A\,(420)}{I_S\,(420)} \times 100\% \tag{1}$$

where I_A and I_S are the integrated intensities of YAG:Ce (420) for precursors calcined at various temperatures for 2 h and the standard samples, respectively.

Fig. 6 shows the crystallinity of the YAG phase in the YAG:Ce nanopowders preparing using different parameters; the average intensity of the (420) diffraction peak was used to analyze the crystallinity of the YAG:Ce nanopowders. The crystallinity of the YAG phase increased concurrently with increases in the calcination temperature. The highest crystallinity of the YAG phase occurred at the stirrer speed of 400 rpm, and the lowest crystallinity of the YAG phase occurred at 500 rpm. This phenomenon may be explained by the finding that the most homogeneous chemical composition of YAG:Ce precursors occurred at 400 rpm.

Fig. 7 represents the morphologies of the YAG:Ce nanopowders for which the precursors were coprecipitated at different electromagnetic stirrer rotational speeds and then heated at 1300 °C. The average particle sizes of the YAG:Ce nanopowders coprecipitated at 200, 300, 400, and 500 rpm were approximately 230, 190, 130, and 220 nm, respectively. The particle size of the YAG:Ce nanopowders decreased when the electromagnetic stirrer rotational speed increased from 200 to 400 rpm. This trend is in agreement with related findings from our previous study [27]. Chen et al. reported that when the stirrer speed was increased to a definite value, the whole reaction zone completely shifted into the plugflow reactor, and the mean particle size decreased to its minimal value. When the stirrer speed was greater than the definite value, a larger mean particle size resulted due to the lower number of nuclei. In sum,

mean particle size increased with increases in the stirrer speed when stirrer speed exceeded the definite value, and mean particle size decreased when the stirrer speed increased below the definite value [31]. In the present study, the average particle size decreased with an increase in the stirrer speed from 200 to 400 rpm, the average particle size then increased when the stirrer speed was increased to 500 rpm. This finding is in agreement with the results of Chen et al. [31].

The luminescence spectra of the YAG:Ce nanopowders synthesized at different stirrer rotation speeds and then calcined at 1300 °C are illustrated in Fig. 8. All the emission spectra of various YAG:Ce nanopowders were detected using a He–Cd laser system with an excitation wavelength of 325 nm. The patterns represent emissions in the range of 400–800 nm, with a maximum luminescence intensity of approximately 540 nm attributed to the Ce^{3+} intershell transition (5d$\rightarrow$4f) in the YAG lattice [32]. The highest intensity emissions were detected in powders synthesized at 400 rpm during the coprecipitation process and calcined at 1300 °C. The fluorescence intensity of this powders was higher than those of commercial YAG:Ce phosphors. Our previous study indicated that a higher rotational speed of the electromagnetic stirrer yields a homogeneously coprecipitated surrounding solution and produces homogeneous precursors, with the Y/Al ratio of the calcined Nd:YAG powders becoming closer to 0.6 [27]. In the present study, the chemical stoichiometry of the YAG:Ce nanopowders was considerably affected by the rotational speed of the electromagnetic stirrer. Fig. 9 presents the photoluminescence spectra of the YAG:Ce precursors synthesized at different rotational speeds of the electromagnetic stirrer and then calcined at different temperatures (900, 1000, 1100, 1200, and 1300 °C). The emission intensities of all the calcined YAG:Ce powders with the precursors prepared at different electromagnetic stirrer rotational speeds increased with the annealing temperature, because of the increase in the crystallinity of the YAG phase [33], and improved the substitution of Ce^{3+} ions into the Y lattice of the YAG matrix; this thus indicates that incorporating Ce^{3+} ions in the YAG matrix improved the emission intensity of the YAG:Ce nanopowders [34,35]. Fig. 10 illustrates the relationships among the average maximum fluorescence intensities of the YAG:Ce nanopowders, stirrer rotation speeds, and calcination temperatures. Across calcination temperatures, the curves indicated that the maximum fluorescence intensity of YAG:Ce nanopowders was the highest at a stirrer speed of 400 rpm, and the maximum fluorescence intensity was significantly lower at the stirrer speed of 200 and 500 rpm. These results correspond with those presented in Fig. 3, 5, and 6; the most homogeneous chemical compositions (Y/Al ratio), phase compositions, and the crystallinities of the YAG phase were all associated with a stirrer speed of 400 rpm, and the aforementioned characteristics corresponded with the highest photoluminescence emissions of YAG:Ce nanopowders. With the exception of the YAG:Ce nanopowders prepared at the stirrer rotation speed of 400 rpm and the calcination temperatures of 1200 and 1300 °C, the fluorescence intensities of others

YAG:Ce nanopowders were significantly lower than those of commercial YAG:Ce phosphors. Fig. 11 presents the average maximum fluorescence intensities of the YAG:Ce precursors prepared at various rotational speeds of the electromagnetic stirrer and then heated at various calcination temperatures. At different stirrer speeds during coprecipitation and then calcination, the average maximum fluorescence intensity of phosphors increased considerably in a range of stirrer speed from 200 to 400 rpm, and the maximum fluorescence intensity significantly reduced at 500 rpm. The average maximum fluorescence intensity of all samples increased as calcination temperatures increased. The maximum average fluorescence intensity was associated with a stirrer speed of 400 rpm. The slopes of fitting lines for the rotational speeds of 200, 300, 400, and 500 rpm were 18.6, 47.1, 65.7, and 18.4, respectively. A high fitting-line slope indicated a high degree of homogeneity in the chemical composition of the precursors. The precursors were precipitated from the mixing solution and were transformed into a single YAG phase, in which the crystalline intensity increased with the calcination temperature (Fig. 6), resulting in a considerable increase in the fluorescence intensity. The results also indicated that during the coprecipitation process, the homogeneity of the chemical composition was reduced at a stirrer speed of 500 rpm.

4. Conclusions

YAG:Ce precursors were synthesized at various electromagnetic stirrer rotational speeds and then calcined at different temperatures to obtain YAG:Ce nanopowders. The crystallinity of the YAG phase within the YAG:Ce nanopowders and the PL emission intensity of the YAG:Ce nanopowders increased with the rotational speed of the electromagnetic stirrer and the calcination temperature. The optimal photoluminescence emission intensity occurred for the YAG:Ce nanopowders with the precursors coprecipitated at 400 rpm and calcined at 1300 °C. This was because of a homogeneous flow field within the mixing solutions, resulting in a high chemical stoichiometry of Y^{3+} and Al^{3+} equal to 3:5 and a higher crystallinity of the YAG phase in the YAG:Ce nanopowders after heating. Moreover, the high quality YAG:Ce nanopowders can be applied in the white LEDs system which can be obtained high luminescent performance.

Reference

[1] Z. Xia, A. Meijerink, Ce^{3+}-Doped garnet phosphors: composition modification, luminescence properties and applications, Chem. Soc. Rev. 46 (2017) 275–299.

[2] S. Nakamura, T. Mukai, M. Senoh, Candela-class high-brightness InGaN/AlGaN double-heterostructure blue-light-emitting diodes, Appl. Phys. Lett. 64 (1994) 1687–1689.

[3] S. Lee, S.Y. Seo, Optimization of yttrium aluminum garnet:Ce^{3+} phosphors for white light-emitting diodes by combinatorial chemistry method, J. Electrochem. Soc. 149 (2002)

85–88.

[4] X. Li, H. Liu, J. Wang, H. Cui, Feng Han, YAG:Ce nano-sized phosphor particles prepared by a solvothermal method, Materials Research Bulletin 39 (2004) 1923–1930.

[5] Z. Wu, X. Zhang, W. He, Y. Du, N. Jia, P. Liu, F. Bu, Solvothermal synthesis of spherical YAG powders via different precipitants, J. Alloy Compd. 472 (2009) 576–580.

[6] X. Zhang, H. Liu, W. He, J. Wang, X. Li, R.I. Boughton, Synthesis of monodisperse and spherical YAG nanopowder by a mixed solvothermal method, J. Alloy Compd. 372 (2004) 300–303.

[7] H. Yang, L. Yuan, G. Zhu, A. Yu, H. Xu, Luminescent properties of YAG:Ce^{3+} phosphor powders prepared by hydrothermal-homogeneous precipitation method, Mater. Lett. 63 (2009) 2271–2273.

[8] X. Li, H. Liu, J. Wang, H. Cui, F. Han, X. Zhang, R.I. Boughton, Rapid synthesis of YAG nano-sized powders by a novel method, Mater. Lett. 58 (2004) 2377–2380.

[9] H. Yang, L. Yuan, G. Zhu, A. Yu, H. Xu, Luminescent properties of YAG:Ce^{3+} phosphor powders prepared by hydrothermal-homogeneous precipitation method, Mater. Lett. 63 (2009) 2271–2273.

[10] L. Wang, H. Kou, J. Li, Y. Pan, J. Guo, Preparation of YAG ceramics through a novel process, Ceram. Int. 38 (2012) 855–859.

[11] Y. You, L. Qi, X. Li, W. Pan, Preparation of YAG nano-powders via an ultrasonic spray co-precipitation method, Ceram. Int. 39 (2013) 3987–3992.

[12] A. Ikesue, T. Kinoshita, K. Kammata, K. Yoshida, Fabrication and optical properties of high-performance polycrystalline Nd:YAG ceramics for solid-state lasers, J. Am. Ceram. Soc. 78 (1995) 1033–1040.

[13] M. Veith, S. Mathur, A. Kareiva, M. Jilavi, M. Zimmer, V. Huch, Low temperature synthesis of nanocrystalline Y$_3$Al$_5$O$_{12}$ (YAG) and Ce-doped Y$_3$Al$_5$O$_{12}$ via different sol–gel methods, J. Mater. Chem. 9 (1999) 3069–3079.

[14] L. Yang, T. Lu, H. Xu, N. Wei, Synthesis of YAG powder by the modified sol–gel combustion method, J. Alloy Compd. 484 (2009) 449–451.

[15] D. Hreniak, W. Strek, Synthesis and optical properties of Nd^{3+}-doped Y$_3$Al$_5$O$_{12}$ nanoceramics, J. Alloy Compd. 341 (2002) 183–186.

[16] G.G. Xu, X.D. Zhang, W. He, H. Liu, H. Li, R.I. Boughton, Preparation of highly dispersed YAG nano-sized powder by co-precipitation method, Mater. Lett. 60 (2006) 962–965.

[17] H. Gong, D. Y. Tang, H. Huang, M. D. Han, T. Sun, J. Zhang, X. P. Qin, J. Ma, Crystallization kinetics and characterization of nanosized Nd:YAG by a modified sol–gel combustion process, Journal of Crystal Growth 362 (2013) 52–57.

[18] P. Ramanujam, B.Vaidhyanathan, J. Binner, A. Anshuman, C. Spacie, A comparative study of the synthesis of nanocrystalline Yttrium Aluminium Garnet using sol-gel and co-precipitation methods, Ceram. Int. 40 (2014) 4179–4186.

[19] L. Wang, H. Kou, Y. Zeng, J. Li, Y. Pan, X. Sun, J. Guo, The effect of precipitant concentration on the formation procedure of yttrium aluminum garnet (YAG) phase, Ceram. Int. 38 (2012) 3763–3771.

[20] H. H. Sheu, S. D. Lin, M. D. Ger, L. C. Chen, Prepared Nd:YAG nano-particles by using co-precipitation process, Journal of Chung Cheng Institute Technology 45 (2016) 64–74.

[21] X. Li , H. Liu, J. Wang, X. Zhang, H. Cui, Preparation and properties of YAG nano-sized powder from different precipitating agent, Optical Materials 25 (2004) 407–412.

[22] Y.H. Lv, W. Zhang, H. Liu, Y.H. Sang, H.M. Qin, J. Tan, L.N. Tong, Synthesis of nano-sized and highly sinterable Nd:YAG powders by the urea homogeneous precipitation method, Powder Technol. 217 (2012) 140–147.

[23] T.M. Chen, S.C. Chen, C.J. Yu, Preparation and characterization of garnet phosphor nanoparticles derived from oxalate coprecipitation, J. Solid State Chem. 144 (1999) 437–441.

[24] M. Zeng, Y. Ma, Y. H. Wang, C. H. Pei, The effect of precipitant on co-precipitation synthesis of yttrium aluminum garnet powders, Ceram. Int. 38 (2012) 6951–6956.

[25] G. Del Rosario, S. Ohara, L. Mancic, O. Milosevic, Characterisation of YAG:Ce powders thermal treated at different temperatures, Applied Surface Science 238 (2004) 469–474.

[26] P. Palmero, C. Esnouf, L. Montanaro, G. Fantozzi, Influence of the co-precipitation temperature on phase evolution in yttrium-aluminium oxide materials, J. Eur. Ceram. Soc. 25 (2005) 1565–1573.

[27] H. H. Sheu, S. Y. Jian, T. T. Lin, Y. W. Lee, Effect of rotational speed of an electromagnetic stirrer on neodymium-doped yttrium aluminum garnet nanoparticle size during co-precipitation, Microelectronic Engineering 176 (2017) 33–39.

[28] C. Marlot, E. Barraud, S. L. Gallet, M. Eichhorn, F. Bernard, Synthesis of YAG nanopowder by the co-precipitation method: Influence of pH and study of the reaction mechanisms, Journal of Solid State Chemistry 191 (2012) 114–120.

[29] Y. Sang, H. Liu, X. Sun, X. Zhang, H. Qin, Y. Lv, D. Huo, D. Liu, J. Wang, R. I. Boughton, Formation and calcination temperature-dependent sintering activity of YAG precursor synthesized via reverse titration method, J. Alloys Compd. 509 (2011) 2407–2413.

[30] M. P. Atkins, C. Bowlas, B. Ellis, F. Hubert, A. Rubatto, P. Wasserscheid, Ionic liquid as catalysts for ethylbenzene production, in: R. D. Rogers, K. R. Seddon, S. Volkov (Eds.), Green industrial applications of ionic liquid, Springer Science Business Media, B.V., Heraklion, 2002, pp. 49-66.

[31] J. Chen, C. Zheng, G. Chen, Interaction of macro- and micromixing on particle size distribution in reactive precipitation, Chemical Engineering Science. 51 (1996) 1957-1966.

[32] C. W. Won, H. H. Nersisyan, H. I. Won, J. H. Lee, K. H. Lee, Efficient solid-state route for the preparation of spherical YAG:Ce phosphor particles, J. Alloys Compd. 509 (2011) 2621–2626.

[33] F. Yuan, H. Ryu, Ce-doped YAG phosphor powders prepared by co-precipitation and heterogeneous precipitation, Materials Science and Engineering B107 (2004) 14–18.

[34] A. B. Ageeth, A. Meijerink, Luminescence quantum efficiency of nanocrystalline ZnS:Mn^{2+}. 1. surface passivation and Mn^{2+} concentration, J. Phys. Chem. B 105 (2001) 10197–10202.

[35] P. Rai, M. K. Song, H. M. Song, J. H. Kim, Y. S. Kim, I. H. Lee, Y. T. Yu, Synthesis, growth mechanism and photoluminescence of monodispersed cubic shape Ce doped YAG nanophosphor, Ceram. Int. 38 (2012) 235–242.
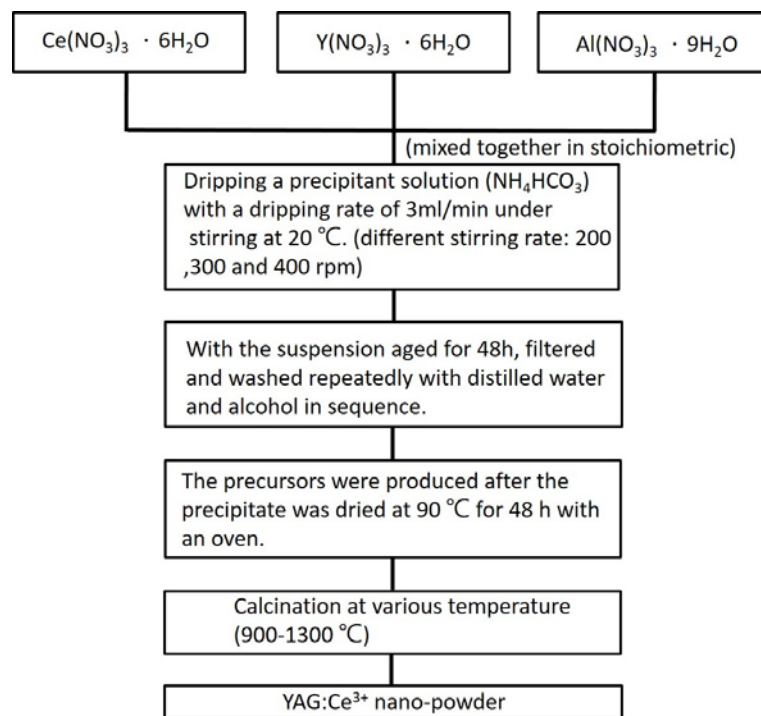
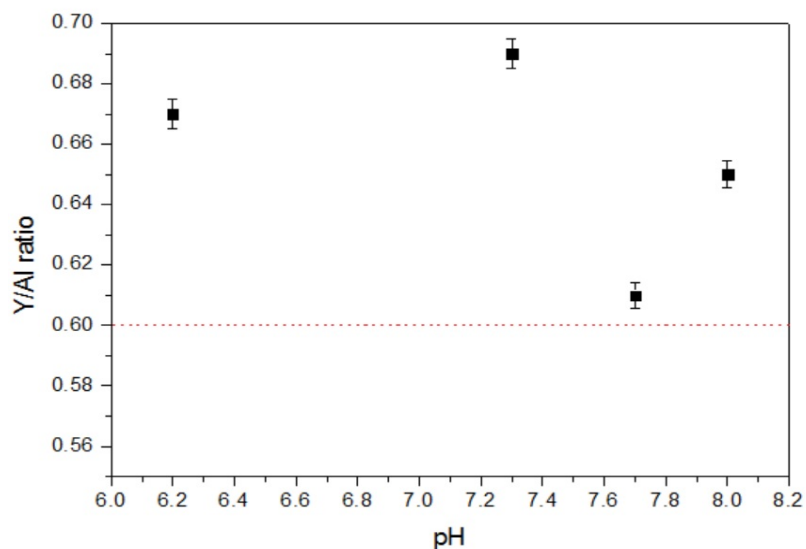Fig. 1. Flowchart of the coprecipitation process for the synthesis of YAG:Ce nanopowders.

Fig. 2. Y/Al ratios of YAG precursors coprecipitated at different pH values and then heated at 1100 °C.
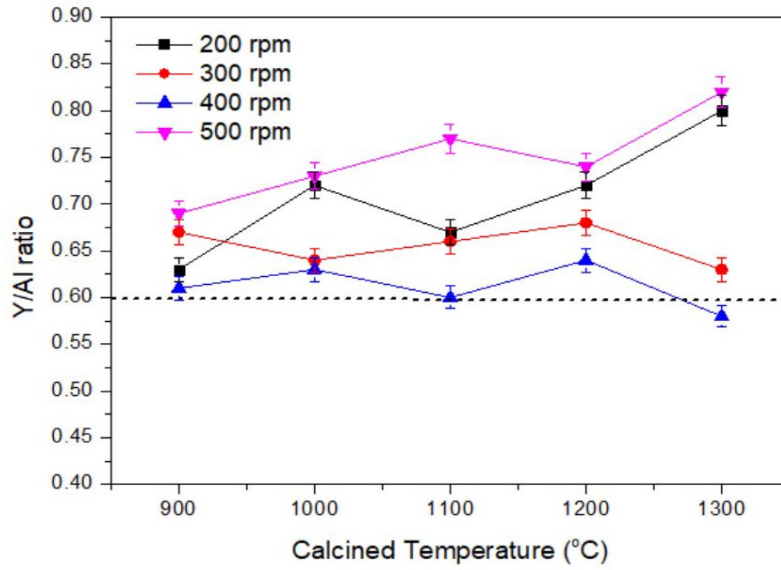
Fig. 3. Y/Al ratios of YAG:Ce precursors coprecipitated at different electromagnetic stirrer rotational speeds and then heated at various calcination temperatures.
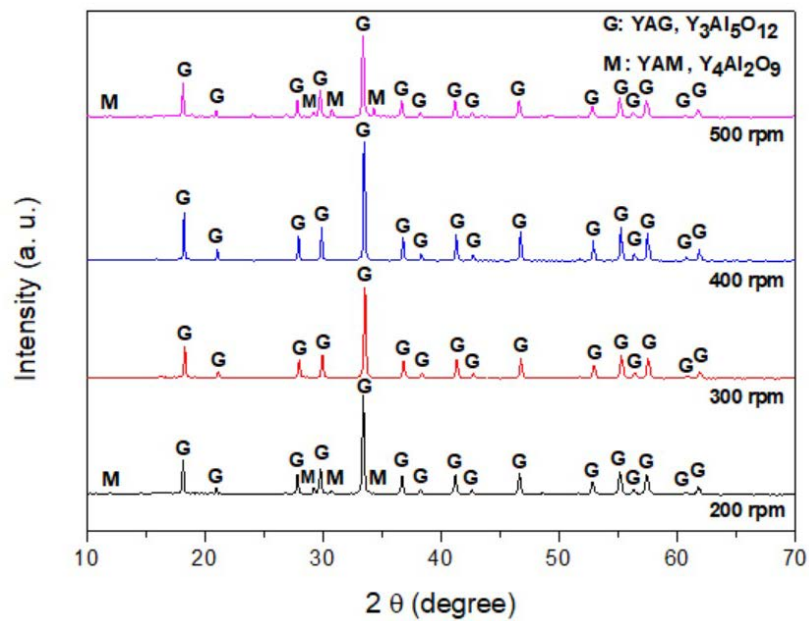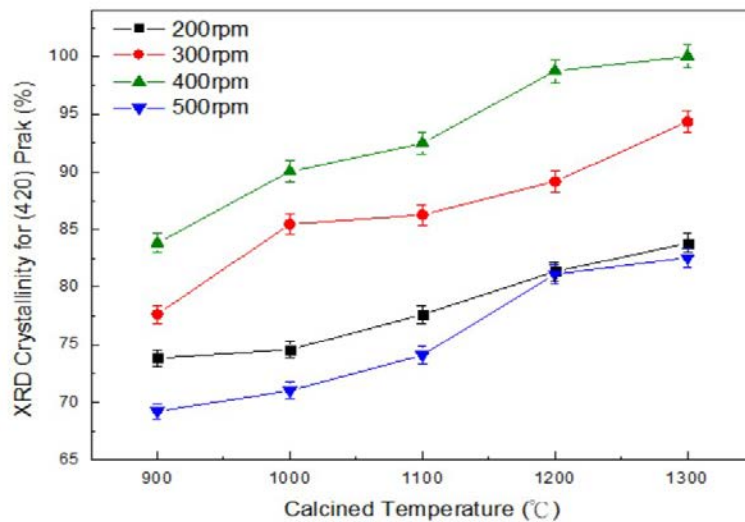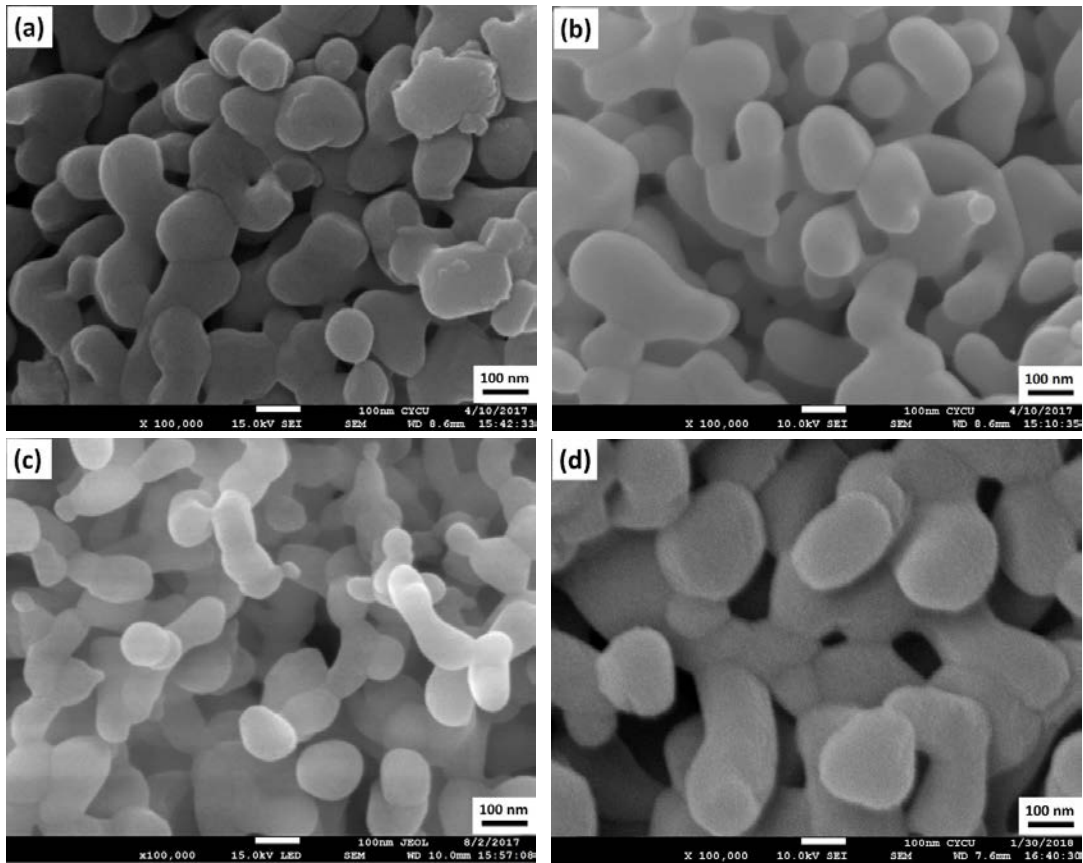

Fig. 4. XRD patterns of YAG:Ce precursors synthesized at different electromagnetic stirrer rotational speeds and then heated at 1300 °C: 200, 300, 400 and 500 rpm.
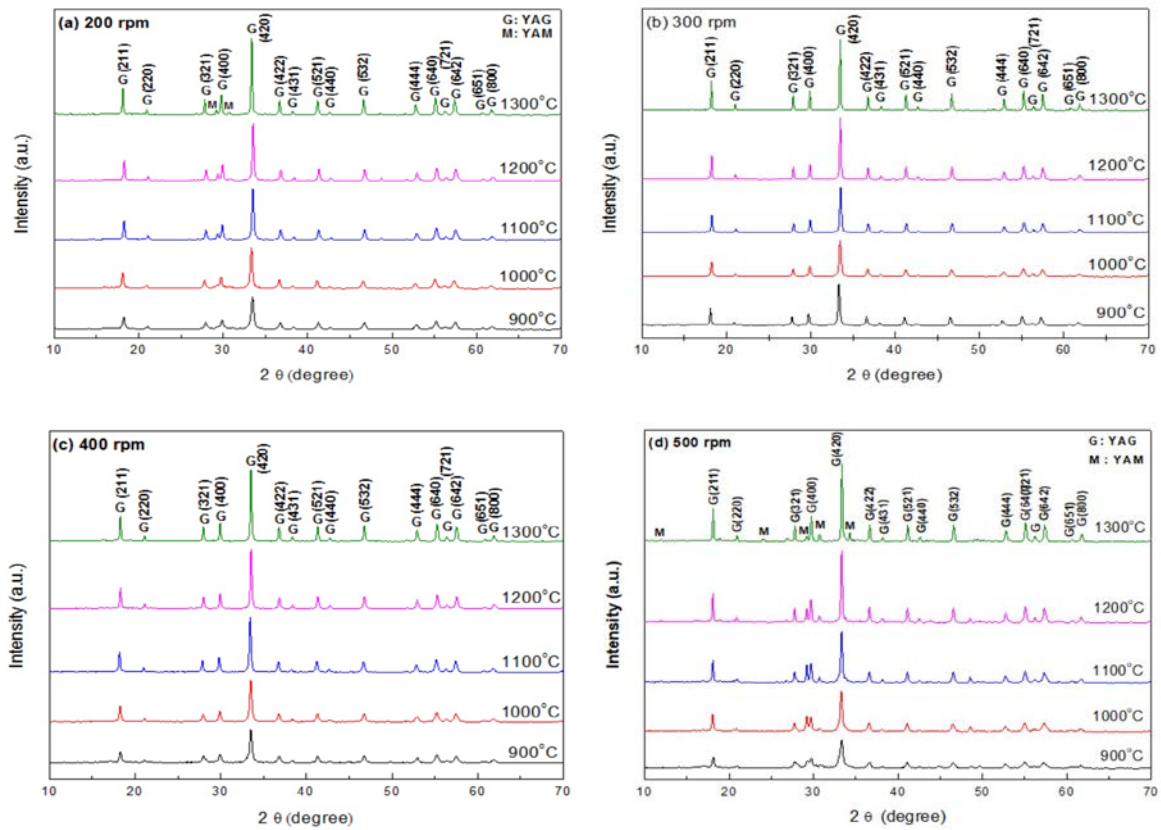
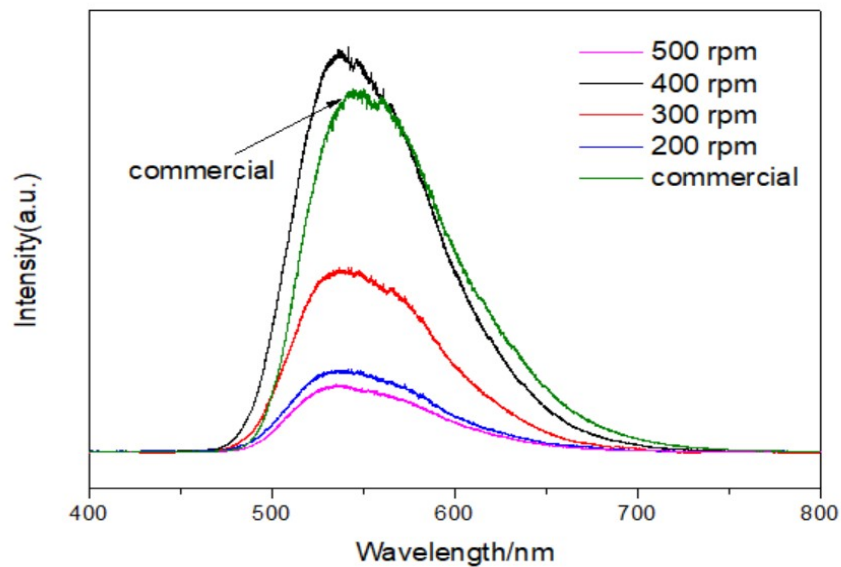Fig. 5. XRD patterns of YAG:Ce precursors synthesized at different electromagnetic stirrer rotational speeds and then heated at various calcination temperatures: (a) 200, (b) 300, (c) 400, and (d) 500 rpm.

Fig. 6. Degree of crystallinity for YAG:Ce precursors synthesized at different electromagnetic stirrer rotational speeds and then heated at different temperatures.

Fig. 7. SEM images of YAG:Ce precursors synthesized at different electromagnetic stirrer rotational speeds and then heated at 1300 °C: (a) 200, (b) 300 (c) 400, and (d) 500 rpm.

Fig. 8. Photoluminescence emission of YAG:Ce nanopowders synthesized at different electromagnetic stirrer rotational speeds and then calcined at 1300 °C (λ_{ex} = 325 nm).
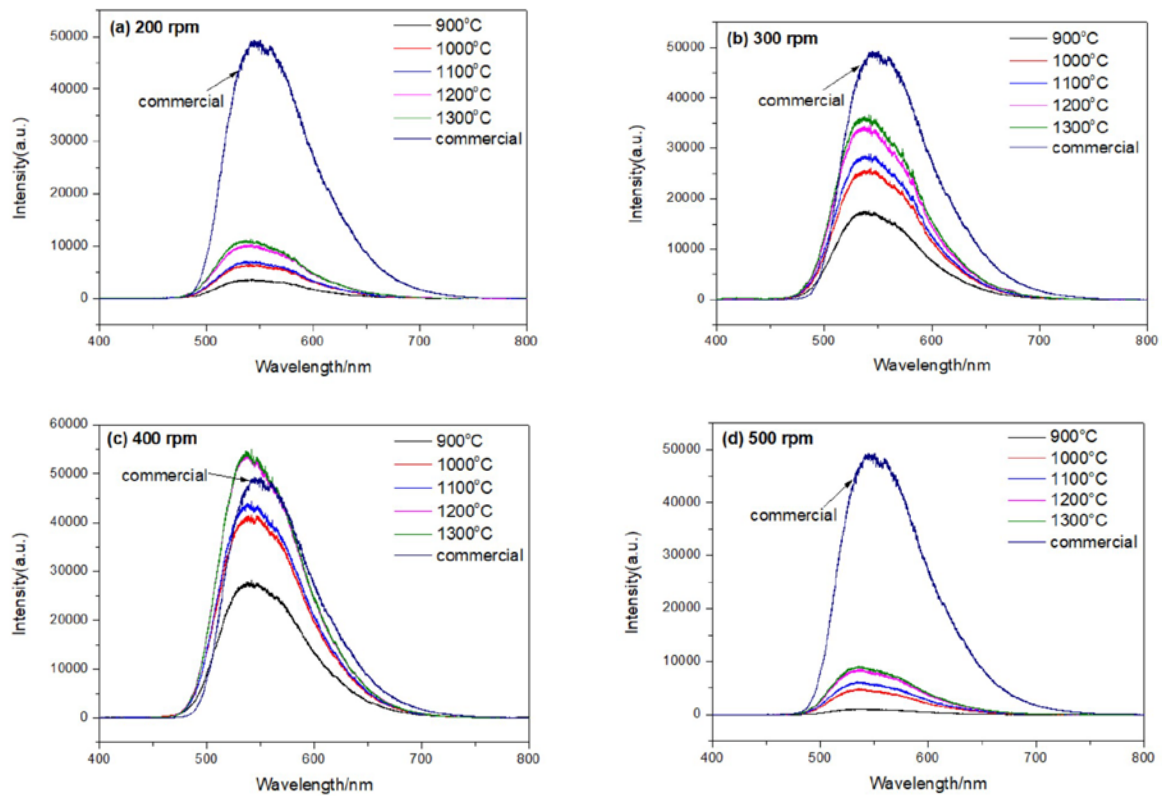
Fig. 9. Photoluminescence emission of YAG:Ce nanopowders synthesized at different electromagnetic stirrer rotational speeds and then heated at various calcination temperatures measured at a wavelength excitation (λ_{ex}) of 325 nm: (a) 200, (b) 300 (c) 400, and (d) 500 rpm.
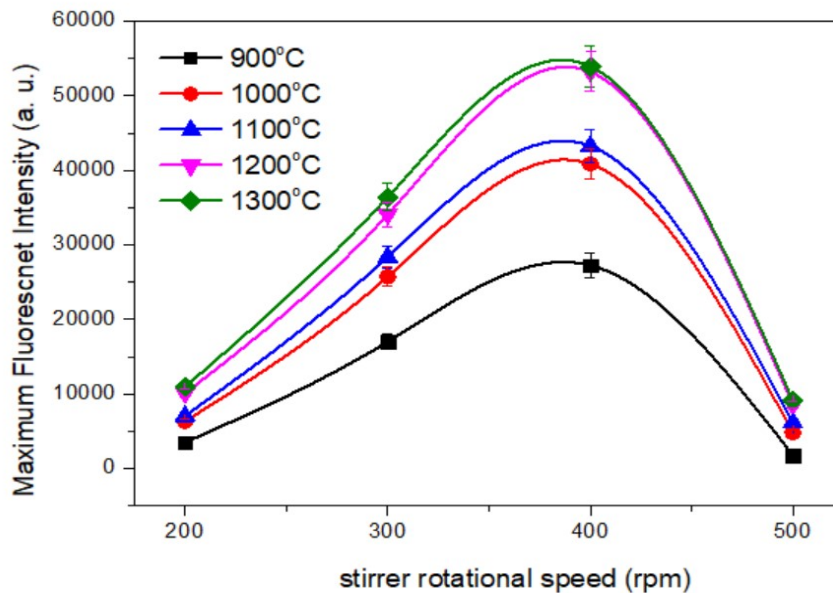

Fig. 10. The relationship between maximum fluorescence intensity of YAG:Ce nanopowders and stirrer rational speed which heated at various calcination temperature.
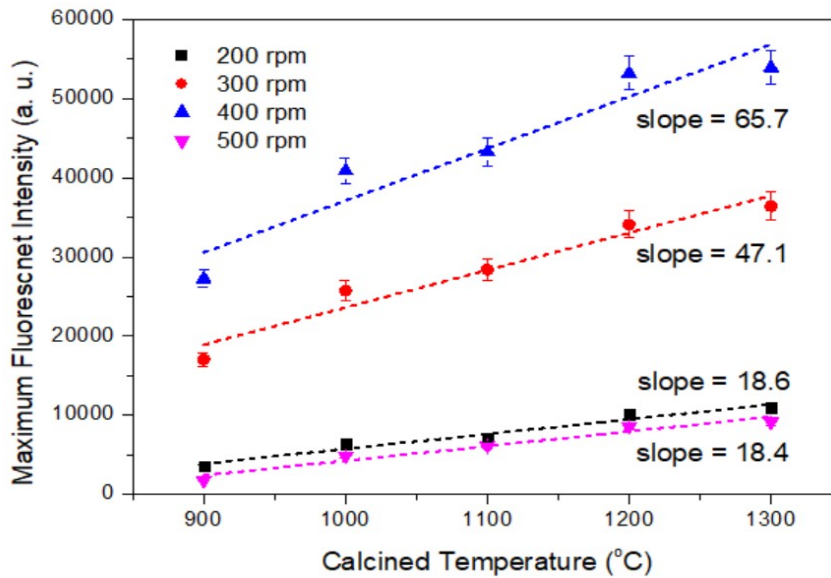
Fig. 11. Maximum fluorescence intensity of YAG:Ce nanopowders synthesized at different electromagnetic stirrer rotational speeds and then heated at various calcination temperatures.

陸、攜回資料（會議議程與摘要集、出席證與註冊證明）